NANOSCALE INVESTIGATION BY SANS OF INCONEL 738 TURBINE BLADES AFTER HIGH-TEMPERATURE OPERATION

MASSIMO ROGANTE[1]*, JAN ŠAROUN[2], PAVEL STRUNZ[2], GIUSEPPE F. CESCHINI[3], VASIL RYUKHTIN[2], PETR LUKÁŠ[2], VOJTĚCH MARINČÁK[2]

[1] *Rogante Engineering Office, NDT, Contrada San Michele n. 61, P.O. Box 189, 62012 Civitanova Marche, Italy*
[2] *Nuclear Physics Institute, 25068 Řež, Czech Republic*
[3] *GEPS Oil & Gas, Nuovo Pignone SPA, via F. Matteucci n. 2, 50127, Firenze, Italy*

Received 3 August 2005, accepted 26 September 2005

Two Inconel 738 nickel-base superalloy gas reactor turbine blades, in as-cast state and after operation, were compared by high-resolution Small Angle Neutron Scattering (SANS) at different positions along their edge, with the aim to assess the influence of high-temperature operation fatigue on the microstructure. Size distributions and relative volume fractions of γ'-precipitates were evaluated from measured SANS spectra for each blade and position.

As results, the precipitate volume fraction increases towards both blades tips. The blade after operation exhibits a significant increase of precipitates average size and volume with respect to the as-cast blade, which can be explained by expected stronger precipitate coarsening under higher stresses. The precipitate size varied along the blade in the as-cast state.

SANS provides a unique possibility of non-destructive characterization of precipitates in the turbine blades. The obtained results confirm the same method as a useful tool for fatigue testing in the considered industrial components.

K e y w o r d s: nickel-base superalloy, precipitation, non-destructive testing, SANS, fatigue

1. Introduction

Due to their attractive properties, nickel-base superalloys [1] offer numerous application possibilities, namely in turbo-machinery industry (jet engines, pump bodies and parts, rocket motors, etc.). These alloys exhibit, in general, a high

*corresponding author, e-mail: engineering@interfree.it

strength together with good oxidation and corrosion resistance. The crucial parameters for their stability at high temperatures are yield stress, high elastic modulus and low thermal expansion coefficient [2, 3]. Outstanding mechanical properties of the same alloys result also from their two-phase structure and strengthening of grain boundaries by carbides. The duplex structure consists of γ' precipitates (FCC ordered $L1_2$ structure) coherently embedded in γ matrix (disordered FCC structure). The high temperature stability and deformation behaviour strongly depend on changes of microstructure caused by complex operating thermo-mechanical conditions [2, 4].

Inconel 738 belongs to modern nickel-base superalloys utilized at high temperatures in aggressive environments, and its microstructure is composed of the Ni-rich γ matrix strengthened by the γ' Ni_3(Al, Ti) and γ'' Ni_3Nb precipitates. The volume fraction of these phases for standard heat treatment ranges from 40 to 43 %. Microstructure control and stabilization is very important for the effective utilization of this superalloy at high temperatures [5].

The Small Angle Neutron Scattering (SANS) method provides information about the microstructure through measuring angular dependence (full scattering angle 2θ) of neutron intensity I scattered by sample to relatively low angles (up to 15°). A quantity independent on the incident flux Φ_0 and on the sample volume V, which is usually used for the characterization of the scattering, is so called differential macroscopic cross section $\mathrm{d}\Sigma/\mathrm{d}\Omega$. It is connected with I by the formula:

$$I(Q) = [\mathrm{d}\Sigma/\mathrm{d}\Omega(Q)] \cdot \Phi_0 \cdot V \cdot T \cdot \Delta\Omega, \tag{1}$$

where $\Delta\Omega$ is the solid angle per detector pixel and T is the sample transmission. The scattering-vector (momentum transfer) magnitude $Q = |\boldsymbol{Q}|$ can be expressed as:

$$Q = |\boldsymbol{Q}| = |\boldsymbol{k} - \boldsymbol{k}_0| = 4\pi \sin\theta/\lambda, \tag{2}$$

where $|\boldsymbol{k}-\boldsymbol{k}_0|$ is the "scattering vector" and λ is the neutron wavelength. If the cross section is drawn in dependence on variable Q (rather than on θ), then its shape and amplitude are independent on the used λ (with exception of the multiple scattering effect not discussed here). $\mathrm{d}\Sigma/\mathrm{d}\Omega(Q)$ contains information about the microstructure of the sample through the Fourier transform. The microstructure is – in case of neutron scattering – represented by the scattering length density (SLD) $\rho(\boldsymbol{r})$ and by the scattering contrast:

$$[\Delta\rho(\boldsymbol{r})]^2 = [\rho(\boldsymbol{r}) - \bar{\rho}]^2, \tag{3}$$

which are analogous to the electron density in the case of X-ray scattering and where $\boldsymbol{r}$ in the expression $\rho(\boldsymbol{r})$ is the size of inhomogeneity (also called "particle").

When a two-phase system without compositional fluctuations is investigated, the scattering contrast simplifies to:

$$[\Delta\rho]^2 = [\rho_{\mathrm{m}} - \rho_{\mathrm{p}}]^2, \tag{4}$$

where ρ_{m} and ρ_{p} are SLDs of the matrix and the precipitates, respectively. It is important to note, that inhomogeneities like γ' precipitates in superalloys have sufficient contrast to give strong intensity (see, e.g., ref. [6]). For the comprehensive review of the SANS theory, see [7] and references therein.

SANS represents a useful tool for non-destructive testing although its full strength has not been employed yet. Some earlier studies of thick samples [8–10] have shown that the non-destructive measurement is feasible and brings useful information on the microstructure. In the present study, SANS method has been used in non-destructive investigation of IN738 superalloy microstructure in real engineering construction components – the gas reactor turbine blades. Two important parameters characterizing the superalloy microstructure were determined at several positions of the blades – the volume fraction and size distribution of the precipitates. The variation of such parameters was measured, with the aim to assess the microstructure response to the thermal fatigue of the examined alloy.

2. Experimental

Table 1 reports the nominal chemical composition [wt.%] of Inconel 738 polycrystalline alloy [5]. The experimental superalloy was thermally treated in two steps: the solution treatment (2 hours at 1120 ℃) was followed by ageing at 845 ℃ for 24 hours. This thermal treatment suppresses γ'' and ensures that only γ' phase is present in the superalloy [4, 5].

Table 1. Nominal chemical composition of Inconel 738 polycrystalline alloy [wt.%]

Ni	Cr	Co	Mo	W	Ta	Al	Ti	C	B	Zr	Nb
Bal.	16.0	8.5	1.7	2.6	1.7	3.4	3.4	0.17	0.01	0.1	0.9

Two turbine blades were investigated, one in the as-fabricated state and the other one after operation. Nine positions along the blade edge (see Fig. 1) were tested by adopting the neutron beam cross-section of (3×15) mm^2. The SANS measurements were carried out at the double-crystal diffractometer DN-2 at NPI Řež (Fig. 2) using the neutron wavelength $\lambda = 0.21$ nm [11]. The adopted instrument allows for measurements with momentum transfers magnitude Q tunable between 0.002 and 0.2 nm^{-1}, which corresponds to the real size range of about 0.01

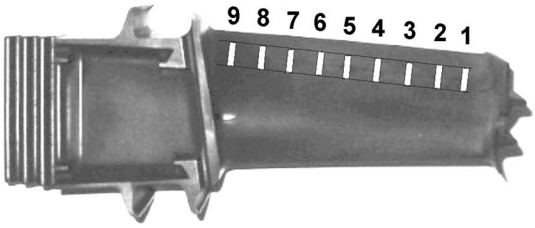

Fig. 1. Turbine blade with marked positions of SANS measurements.

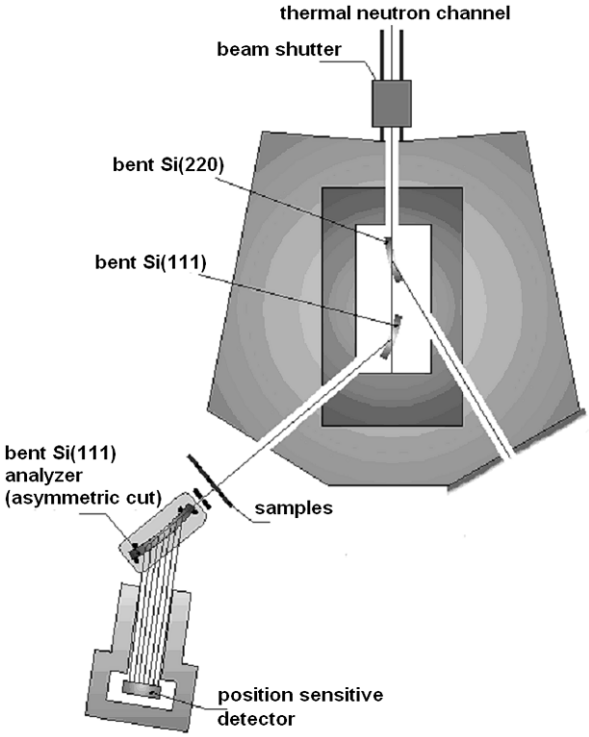

Fig. 2. Scheme of the DN-2 SANS facility at LVR-15 reactor in Řež.

to 1 μm. The resolution of the same instrument can be properly tuned by elastic bending of the monochromator and analyzer crystals. In our case, measurements were carried out in two overlapping Q ranges of 0.02–0.16 nm^{-1} and 0.008–0.07 nm^{-1}, respectively.

3. Data evaluation and results

Two separate evaluation procedures were used for the extraction of the real-space information from the measured data: Guinier approximation and the model fitting.

3.1 Guinier approximation

The low-Q region of SANS data provides information about the size of large precipitates, namely their radius of gyration, R_g. For $Q \leq 1/R_g$, the scattering curve $S(Q)$ can be described by the Guinier approximation, which is expressed for pin-hole geometry by the relation:

$$\ln S(Q) \approx \ln S(0) - \frac{1}{3}(R_g Q)^2. \tag{5}$$

The resolution of double-crystal instruments is adequately described by so-called infinite-slit geometry, where the approximation (5) still holds, but Q has the meaning of the horizontal component of the momentum transfer Q_x and R_g has to be replaced by a slightly different value R_{g_slit},

$$R^2_{g\_slit} = \frac{14}{15} R^2_g, \tag{6}$$

as can be easily proved. The low-Q ranges of scattering curves were therefore fitted by the polynomial:

$$\ln S(Q_x) = A + \frac{1}{3} R^2_{g\_slit} Q^2_x + C Q^4_x, \tag{7}$$

where the third term was used to account for higher order of the approximation (5), see Fig. 3. Resulting radius of gyration was recalculated to an effective sphere radius using the relation:

$$R_{sphere} = \sqrt{\frac{5}{3}} R_g. \tag{8}$$

The value of scattering cross-section in the forward direction, $S(0)$, in the infinite-slit geometry is proportional to volume fraction multiplied by the square of the particle size. Relative volume fractions were therefore calculated as $S(0)/R^2$ (see Fig. 4).

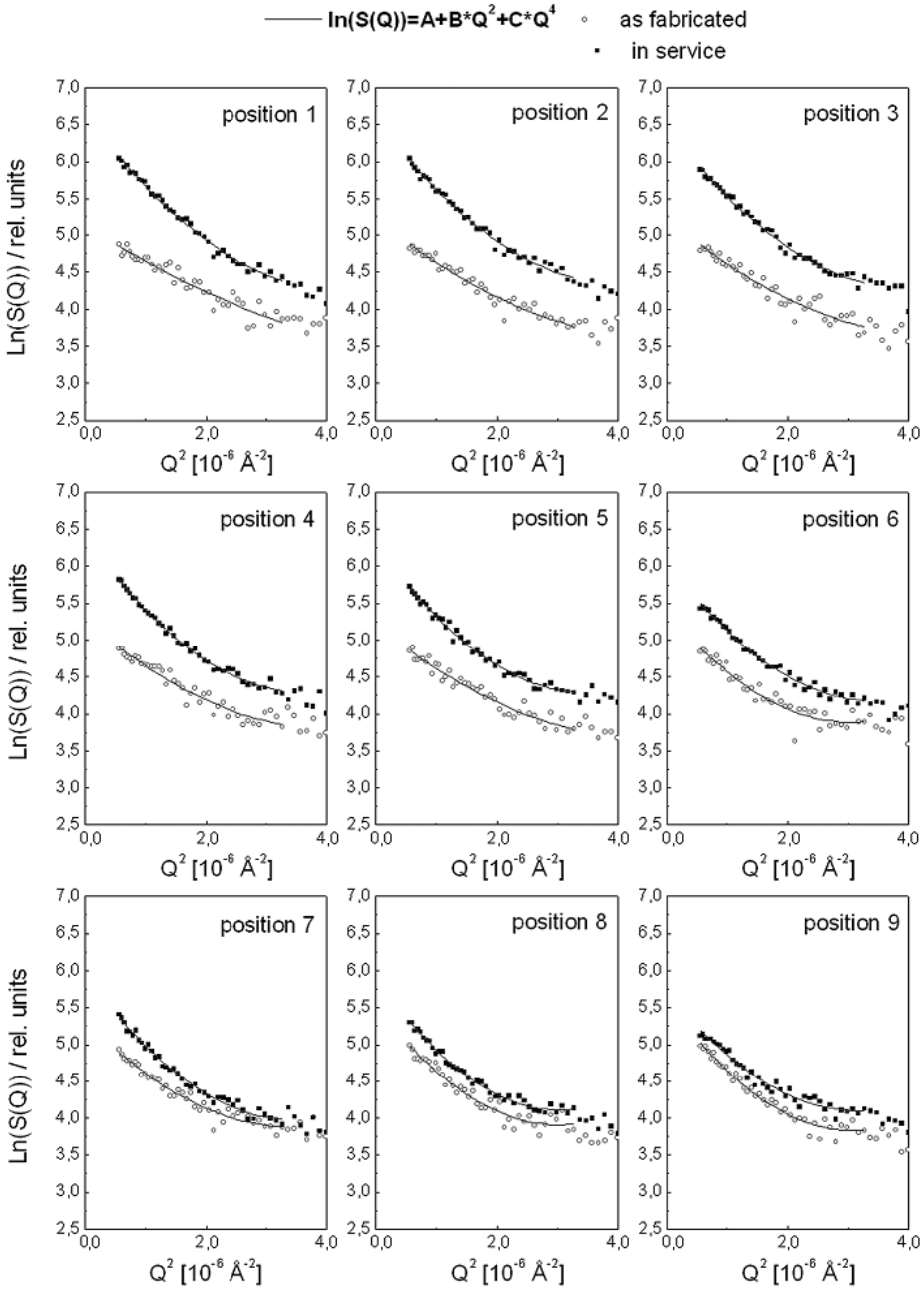

Fig. 3. Guinier plots of the SANS data at the low-Q part of the scattering curves.

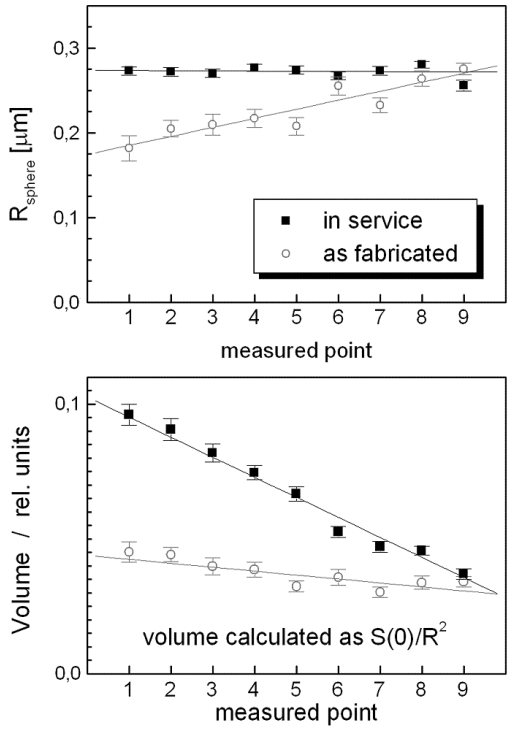

Fig. 4. Effective sphere radii and volume fractions evaluated from Guinier approximation at small momentum transfers.

3.2 Model of spherical precipitates

The used model consists of two sets of spherical particles with size distributions represented by cubic splines. The two sets were defined on different size ranges of 4–80 nm and 80–400 nm represented thus small and large particles, respectively. The maximum sizes were further adjusted as free parameters during the data fitting. The description of precipitates shape by spheres is adequate if one wants to evaluate the mean size averaged over the variety of particle shapes and orientations within the large gauge volume. Moreover, a secondary precipitation exists in the investigated material, as shown in Fig. 5. The size distributions resulting from the fit are shown in Fig. 6. The integration over R-range gives the volume fraction in the given range. As the size distributions were defined on the logarithmic scale in R, the integrated volume fractions of large particles (see Fig. 7) are much higher than it may seem from the graphs without any scaling. Size distributions for small

particles were thus scaled by factor 1/25 in Fig. 5, so that they can be displayed in the same graph as the large ones.

4. Discussion and conclusions

The large precipitates volume fraction increases towards the tip for the used blades (Fig. 7). This effect can be explained by the coarsening of smaller precipitates and/or by their coalescence into larger structures (rafting). This process is most pronounced at the blade tip (point 1) exposed to high temperatures, indicated, e.g., by creation of 0.1 mm oxide coat. In contrast to this fact, the mean size of large precipitates in the non-used blade decreases towards the blade tip (Fig. 4). The possible explanation can be found in the thermal treatment during the fabrication process. The turbine blades are heated at high temperatures for relatively long time. During this holding time, particles are partially dissolved and the solid solution is saturated. After that, by the cooling, the precipitates grow from the saturated solution, but the cooling is too fast and the particles mean size is lower than before. This process, of course, is most intensive at the blade tip, due to the faster cooling of smaller volume at the same position.

The adopted microstructural model neglects any effects of interparticle interference due to the short-range ordering of the γ' precipitates, such ordering being typical for the same precipitates. Owing to the large interparticle distances, this effect is significant mainly at small Q values below the limit of our measurement. Nevertheless, small bias caused by the precipitates ordering is possible.

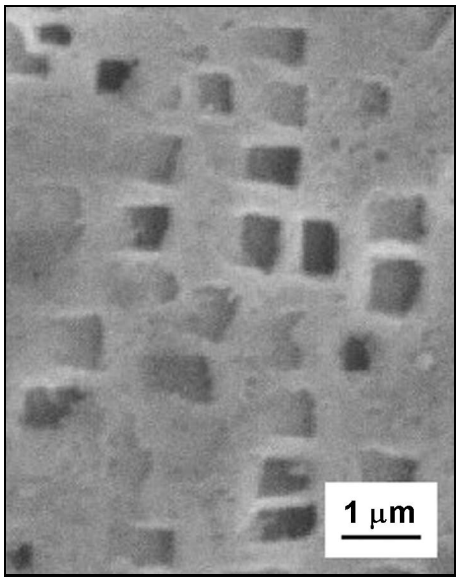

Fig. 5. Inconel 738 γ' phase at blade root (Molybdic acid 50 %).

The particles growth at the blade tip (Fig. 4) during operation is probably caused by high temperature levels, which induce a coarsening of turbine microstructure and a growth of the precipitates. The particles size, then, is approximately the same along the whole turbine blade. The resulting microstructural parameters could be influenced, obviously, also by the inhomogeneous distribution of stresses and temperatures along the turbine axis and along the turbine cross-section after operation.

The big difference between the scattering power, which is manifested by the difference in apparent volume

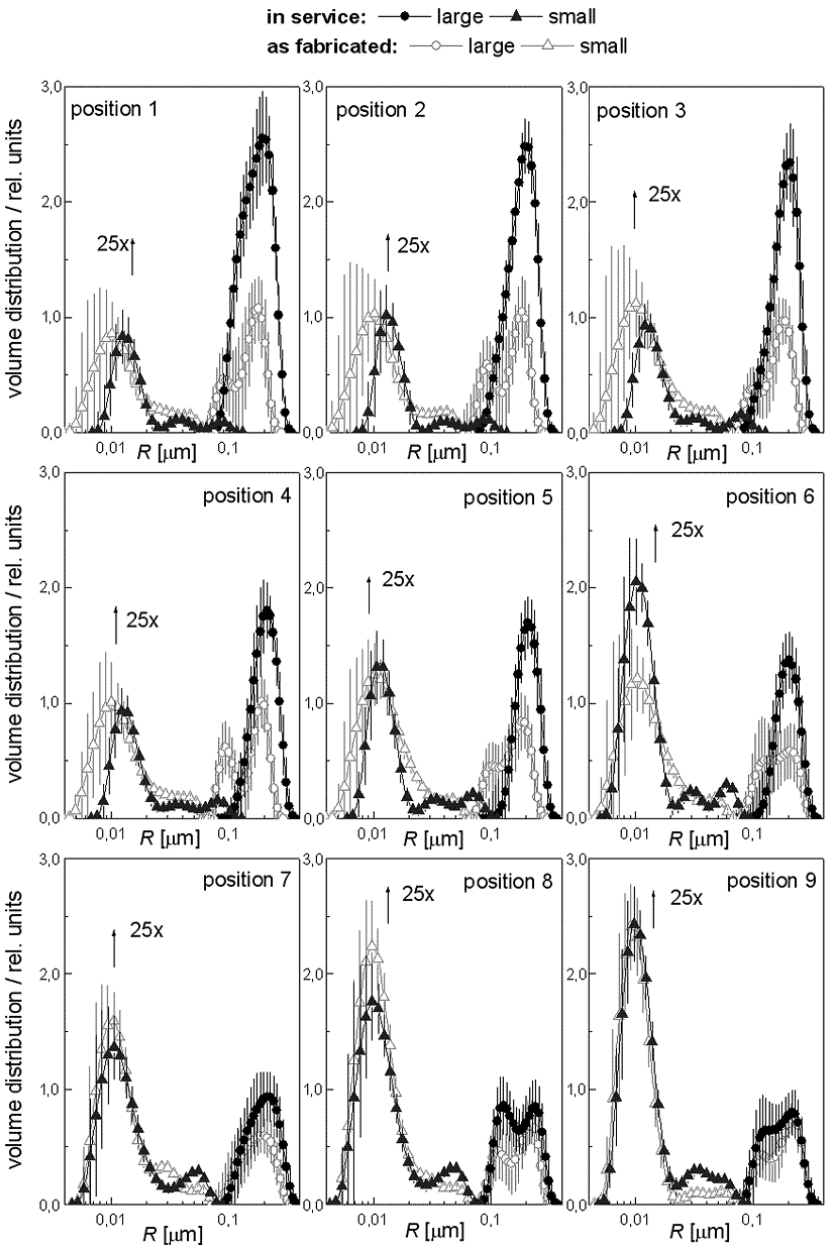

Fig. 6. Size distributions evaluated from SANS data measured at the nine positions along the blades. Note the scaling factor used to plot the distributions of small particles and logarithmic R-scale.

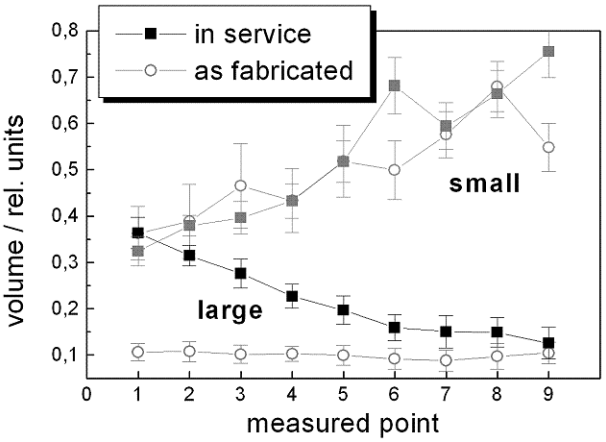

Fig. 7. Integrated volume fractions (in relative units) of large and small precipitates.

fractions, indicates that there are two different phases contributing to the scattering. In Fig. 5, the ratio of sizes primary/secondary precipitates can be estimated to be roughly 10. It fully corresponds to the Fig. 6, indicating that the model of primary and secondary gamma prime precipitates well describes the observed scattering curves.

The model of spheres is, of course, too simple to describe all precipitates which can be present in the material. The peak at small radii just reveals that there are objects of small dimension present in the material, but we cannot decide whether we see very small round precipitates or just the thickness of larger but thin plate-like precipitates. An independent determination of scattering contrast of the precipitates allows to better identify the phases, which contribute predominantly to the scattering in both large- and small-Q regions, to determine the volume fractions on absolute scale and to exclude the eventual presence of small voids.

The porosity in the oxide layer and/or the blade itself, finally, could contribute to the scattering; hopefully, this contribution is not significant, and its estimation needs a guess of the pores volume fraction and size – the observable pores are quite large, around 10 micrometers – and the oxide layer composition.

The high-resolution SANS measurements, in conclusion, seem to be very prospective as a non-destructive method for the assessment of turbine blade degradation during operation. The parameters like mean radius of gyration and volume fraction can be almost certainly used as adequate quantities, which reflect the degradation level.

Acknowledgements

The work was supported through the projects MSM 2672244501 and IRP AV0Z10480505.

REFERENCES

[1] DURAND-CHARRE, M.: The Microstructure of Superalloys. Amsterdam, Gordon and Breach Science Publishers 1997.
[2] KHAN, T.—CARON, P.: In: High Temperature Materials for Power Engineering. Part II. Eds.: Bachelet, E. et al. Dordrecht, The Netherlands, Kluwer Academic Publisher 1990, p. 1261.
[3] CURTIS, R. V.—GHOSH, R. N.—Mc LEAN, M.: In: Proceedings of the Fifth International Conference. Eds.: Wilshire, B., Evans, R. W. London, Institute of Materials 1993, p. 199.
[4] ZRNÍK, J.: Influence of thermal and stress loading on the structure of nickel superalloys. [Habilitation Thesis]. Department of Material Sciences, Technical University of Košice, Slovakia 1990, p. 15.
[5] FRENZ, H.—MEERSMANN, J.—ZIEBS, J.—KÜHN, J.—SIEVERT, R.— OLSCHEWSKI, J.: Mat. Sci. and Engineering, *A 230*, 1997, p. 49.
[6] STRUNZ, P.—MUKHERJI, D.—GILLES, R.—RÖSLER, J.—WIEDENMANN, A.: Mat. Sci. Forum, *426–432*, 2003, p. 821.
[7] KOSTORZ, G.: In: Neutron Scattering (Treatise on materials science and technology). Ed.: Kostorz, G. New York, Academic Press 1979, p. 227.
[8] STRUNZ, P.—ZRNÍK, J.—GILLES, R.—WIEDENMANN, A.: Physica B, *276-278*, 2000, p. 890.
[9] STRUNZ, P.—LUKÁŠ, P.—MIKULA, P.—ŠAROUN, J.—KEILOVÁ, E.—KOČÍK, J.: Acta Physica Hungarica, *75*, 1994, p. 279.
[10] ROGANTE, M.—LEBEDEV, V. T.: Nanoscale investigation by SANS of Inconel 738 samples submitted to different ageing treatments, manuscript in preparation.
[11] STRUNZ, P.—ŠAROUN, J.—MIKULA, P.—LUKÁŠ, P.—EICHHORN, F.: J. Appl. Cryst., *30*, 1997, p. 844.